Selective blockade of T lymphocyte K^+ channels ameliorates experimental autoimmune encephalomyelitis, a model for multiple sclerosis

Christine Beeton*†, Heike Wulff†‡, Jocelyne Barbaria*, Olivier Clot-Faybesse*, Michael Pennington§, Dominique Bernard*, Michael D. Cahalan‡¶, K. George Chandy‡, and Evelyne Béraud*

*Laboratoire d'Immunologie, Faculté de Médecine, 13385 Marseille, France; ‡Department of Physiology and Biophysics, University of California, Irvine, CA 92697; and §Bachem Bioscience, King of Prussia, PA 19406

Communicated by Clay M. Armstrong, University of Pennsylvania School of Medicine, Philadelphia, PA, September 18, 2001 (received for review June 6, 2001)

Adoptive transfer experimental autoimmune encephalomyelitis (AT-EAE), a disease resembling multiple sclerosis, is induced in rats by myelin basic protein (MBP)-activated $CD4^+$ T lymphocytes. By patch-clamp analysis, encephalitogenic rat T cells stimulated repeatedly *in vitro* expressed a unique channel phenotype (''chronically activated'') with large numbers of Kv1.3 voltage-gated channels (≈1500 per cell) and small numbers of IKCa1 Ca^{2+}-activated K^+ channels (≈50–120 per cell). In contrast, resting T cells displayed 0–10 Kv1.3 and 10–20 IKCa1 channels per cell (''quiescent'' phenotype), whereas T cells stimulated once or twice expressed ≈200 Kv1.3 and ≈350 IKCa1 channels per cell (''acutely activated'' phenotype). Consistent with their channel phenotype, [^{3}H]thymidine incorporation by MBP-stimulated chronically activated T cells was suppressed by the peptide ShK, a blocker of Kv1.3 and IKCa1, and by an analog (ShK-Dap^{22}) engineered to be highly specific for Kv1.3, but not by a selective IKCa1 blocker (TRAM-34). The combination of ShK-Dap^{22} and TRAM-34 enhanced the suppression of MBP-stimulated T cell proliferation. Based on these *in vitro* results, we assessed the efficacy of K^+ channel blockers in AT-EAE. Specific and simultaneous blockade of the T cell channels by ShK or by a combination of ShK-Dap^{22} plus TRAM-34 prevented lethal AT-EAE. Blockade of Kv1.3 alone with ShK-Dap^{22}, but not of IKCa1 with TRAM-34, was also effective. When administered after the onset of symptoms, ShK or the combination of ShK-Dap^{22} plus TRAM-34 greatly ameliorated the clinical course of both moderate and severe AT-EAE. We conclude that selective targeting of Kv1.3, alone or with IKCa1, may provide an effective new mode of therapy for multiple sclerosis.

Multiple sclerosis (MS), a chronic inflammatory autoimmune disease of the central nervous system that commonly affects young adults, is characterized by demyelination and axonal damage resulting in disabling neurologic deficits (1). Experimental autoimmune encephalomyelitis (EAE) mimics many of the clinical and pathological features of MS and is widely used as a model for the human disease (2–4). The central role of T lymphocytes in pathogenesis is demonstrated by the induction of adoptive transfer (AT)-EAE in naive animals after adoptive transfer of myelin basic protein (MBP)-activated $CD4^+$ T cells (2, 3, 5–7). Strategies designed to selectively suppress the function of autoreactive T cells represent a potential therapeutic approach for MS.

Optimal T cell activation requires several hours of calcium entry from the external milieu through Ca^{2+} release-activated Ca^{2+} (crac) channels (8–10). Ca^{2+} influx depolarizes the membrane and dissipates the electrochemical gradient required for further Ca^{2+} entry. Two K^+ channels, Kv1.3 and IKCa1, provide the counterbalancing cation efflux necessary for sustained Ca^{2+} influx (10). Kv1.3, a voltage-gated channel, opens in response to membrane depolarization and maintains the resting membrane potential, whereas IKCa1 opens in response to an increase in cytosolic Ca^{2+} and hyperpolarizes the membrane potential (11). Kv1.3 is found in the hematopoietic lineage, including T and B lymphocytes, platelets and megakaryocytes, and microglia, whereas the distribution of IKCa1 is broader, including a variety of peripheral tissues and cell types (9, 12, 13). Kv1.3 is the primary regulator of Ca^{2+} signaling in human quiescent T cells. Selective blockade of Kv1.3, but not IKCa1, suppresses mitogen-stimulated cytokine production and proliferation of these cells *in vitro* (14–17) and the delayed type hypersensitivity response *in vivo* (6, 18, 19). Transcriptional up-regulation during mitogenesis results in IKCa1 becoming the main regulator of Ca^{2+} signaling in human activated lymphocytes, and selective IKCa1 blockade suppresses cytokine production and mitogenesis of preactivated cells (17, 20, 21). Because of their important role in T cell activation (9), adhesion, and migration (22), and their functionally restricted distribution, both channels are widely regarded as novel therapeutic targets.

Kaliotoxin (KTX), a peptide from scorpion venom that blocks the lymphocyte Kv1.3 and the neuronal Kv1.1 channels, ameliorates the symptoms of adoptive EAE in rats (6). Its therapeutic effect may be due to immunosuppression via Kv1.3 blockade, or to enhanced nerve conduction via blockade of Kv1.1, or to a combination of both. In the present study, we tested whether selective *in vivo* blockade of the T cell K^+ channels could prevent and treat adoptive EAE in Lewis rats. ShK, a structurally defined 35-aa polypeptide from the sea anemone *Stichodactyla helianthus*, was used to inhibit both Kv1.3 (K_d = 11 pM) and IKCa1 (K_d = 20 nM). However, this polypeptide also blocks Kv1.1 (K_d = 16 pM), Kv1.4 (K_d = 314 pM), and Kv1.6 (K_d = 160 pM). Based on sequence differences in these channels, we previously engineered ShK-Dap^{22} to be a highly potent (K_d = 20–50 pM) and specific (16, 17, 23) inhibitor of Kv1.3. We used ShK-Dap^{22} to selectively target Kv1.3 and the clotrimazole analog TRAM-34 (K_d = 20 nM) as a selective blocker of IKCa1 (21). By whole-cell patch-clamp, we demonstrate that rat T cell lines or clones that have been repeatedly stimulated with MBP or other antigens exhibit a unique K^+ channel phenotype different from that of normal quiescent or acutely activated rat T cells. Guided by these patch clamp results and by data from *in vitro* proliferation assays, we have successfully prevented lethal AT-EAE and significantly ameliorated the disease when starting treatment after onset of symptoms.

Abbreviations: MBP, myelin basic protein; EAE, experimental autoimmune encephalomyelitis; MS, multiple sclerosis; K_{Ca}, Ca^{2+}-activated K^+ channel; K_v, voltage-gated potassium channel; [^{3}H]TdR, tritiated thymidine; Mt, *Mycobacterium tuberculosis*; PPD, purified protein derivative of tuberculin; AT, adoptive transfer; KTX, kaliotoxin; MgTX, margatoxin; ChTX, charybdotoxin; TRAM-34, [1-(2-chlorophenyl)diphenylmethyl]-1*H*-pyrazole.

†C.B. and H.W. contributed equally to this work.

¶To whom reprint requests should be addressed. E-mail: mcahalan@uci.edu.

The publication costs of this article were defrayed in part by page charge payment. This article must therefore be hereby marked "*advertisement*" in accordance with 18 U.S.C. §1734 solely to indicate this fact.

Materials and Methods

Animals. Female inbred Lewis rats 8–12 weeks of age and guinea pigs were purchased from Harlan Breeding Laboratories (Gannat, France).

Reagents. ShK, ShK-Dap^{22}, margatoxin (MgTX), KTX, and charybdotoxin (ChTX) were from Bachem (King of Prussia, PA) or from Alomone Laboratories (Jerusalem, Israel). Synthesis of TRAM-34 ([1-(2-chlorophenyl)diphenylmethyl]-1*H*-pyrazole) was previously described (21). Tetraethylammonium, clotrimazole, PHA, and Con A were purchased from Sigma, purified protein derivative of tuberculin (PPD) from Statens Serum Institut (Copenhagen), complete Freund's adjuvant and *Mycobacterium tuberculosis* H37 Ra (Mt) from Difco, and anti-CD4 Ab from Serotec. MBP was extracted from frozen guinea pig central nervous system (24), purified by C18 reverse-phase HPLC (Millipore/Waters system), and purity was assessed by electrospray mass spectrometry.

Cells and Cell Lines. PAS T cells, MHC class II-restricted CD4$^+$ T cells, are encephalitogenic *in vivo* and produce limited demyelination (25, 26). PAS and other MBP-specific T cell lines and clones were previously established from MBP-primed rat lymph nodes from Lewis (CB, E10, LEG, Z, ZNP, MBP-33, LR88L1, BP10-S5, 71S5, Go1-S3, Go3-S3), DA (DAG), or Fisher (Fisher S5) strains. The clones/lines Z, ZNP, A2b (Mt-specific), BP10-S5, 71S5, Go1-S3, Go3-S3, and Fisher S5 were gifts from A. Ben-Nun, I. Cohen, and F. Mor (Weizmann Institute of Science, Rehovot, Israel). MBP-33 (27) and OVA-Jung (ovalbumin-specific) were gifts from S. Jung (University of Würzburg, Germany), LR88L1 was a gift from J. Whitaker (University of Alabama, Birmingham, AL), and DAG and LEG were gifts from D. Hinrichs (Oregon Health Sciences University, Portland, OR). MBP-specific T cells (3×10^5/ml) were incubated for 2 days with 10 μg/ml of MBP and 15×10^6/ml syngeneic irradiated (3000 rad) thymocytes as antigen presenting cells in RPMI 1640 Dutch modification medium supplemented with 1% homologous rat serum and additives (stimulation medium, ref. 23). The same conditions of activation were applied to A2b (25 μg/ml Mt) and to PPD-T cells (20 μg/ml PPD). Mononuclear cells were isolated from spleens and enriched for T cells (>90% CD3$^+$ cells) by nylon wool. CD4$^+$ T cells from lymph nodes were isolated by using a MiniMACS cell sorter (Miltenyi Biotec, Paris).

[^{3}H]Thymidine ([^{3}H]TdR) Incorporation Assays. Resting or 2-day-activated (5 μg/ml Con A) T cells were seeded at 2×10^5 cells per well in culture medium in flat-bottom 96-well plates (final volume 200 μl). After 4–6 days of IL-2-dependent expansion, PAS T cells were seeded in stimulation medium in the presence of antigen-presenting cells. Cells were preincubated with K$^+$ channel blockers for 60 min and then stimulated with the mitogen Con A (2 μg/ml) for 48 h or the specific antigen MBP (5 μg/ml) for 72 h. [^{3}H]TdR (1 μCi per well) was added for the last 6 to 16 h. Cells were harvested onto glass fiber filters, and radioactivity was measured in a β-scintillation counter.

Electrophysiological Analysis. All experiments were conducted in the whole-cell configuration of the patch-clamp technique as described (21).

Prevention and Treatment of AT-EAE in Lewis Rats. In the AT-EAE model, two phases are required for disease induction: an *in vitro* sensitization phase, in which T cells are challenged with autoantigen and become encephalitogenic, followed by an effector phase, in which the adoptively transferred cells home to the central nervous system and cause disease. For the prevention trial, we set up conditions to ensure that channel blockers were continuously present during both phases. PAS T cells were stimulated with MBP for 48 h in the presence or absence of channel blockers (100 nM ShK, 100 nM ShK-Dap^{22}, 500 nM TRAM-34, or 100 nM ShK-Dap^{22} + 500 nM TRAM-34) or PBS. Cells were washed, viability was assessed by trypan blue dye exclusion, and 4–5.5 $\times$ 10^6 viable cells in 1 ml RPMI medium 1640 were transferred i.p. into four treatment groups of syngeneic rats and into a saline (PBS + 2% Lewis rat serum) control group. Soon after, the four groups received i.p. injections of the same K$^+$ channel blocker(s) used during the sensitization activation step: 16 μg ShK or ShK-Dap^{22} in 0.5 ml saline (80 μg/kg), or 34 μg TRAM-34 (170 μg/kg) in 0.1 ml of a 50:50 mixture of PBS:DMSO or alcohol or a combination of ShK-Dap^{22} and TRAM-34. The protocol was continued with three more injections at 4-hr intervals on day 0, three injections on day 1, and two injections on days 2–5. Control animals received saline injections with the same protocol. Rats were weighed and observed daily.

For the treatment trials, blockers were administered exclusively *in vivo* and after the onset of disease. After the sensitization step (cells *in vitro* activated with MBP for 48 h), 3–5 $\times$ 10^6 viable PAS T were injected i.p. into syngeneic rats. Because encephalitogenic potency varied from batch to batch, we adjusted the number of cells transferred in each experiment to induce disease of differing severity. Therapy with ShK, ShK-Dap^{22} + TRAM-34, or saline (i.p.) was started immediately after the first clinical signs of EAE were observed. The animals received four injections during the first 24 h, three injections during the second 24 h, and two injections during the third 24-h period.

Results

Identification of Kv1.3 and IKCa1 Channels in PAS T Cells. By using established protocols during whole-cell recording, we characterized K$^+$ channels of the encephalitogenic CD4$^+$, CD25^{hi}, CD44^{hi}, CD18^{hi}, CD45RA$^-$, MBP-specific PAS long-term T cell line. These cells display a very large voltage-gated K$^+$ (K_V) current with a biophysical and pharmacological "fingerprint" indistinguishable from that of the Kv1.3 channel described previously in human and mouse T cells and in expression systems (28–30). Depolarizing voltage steps typically elicited a family of K$^+$ currents with a half-activation voltage of -33 mV (Fig. 1*A*) and τ_n of 2.6 $\pm$ 0.5 ms (at 40 mV). Repetitive depolarizing pulses to 40 mV progressively reduced the current amplitude (Fig. 1*B*), a "use-dependent" inactivation that is characteristic of Kv1.3 (9, 28–30). During a long depolarizing pulse to 40 mV, the current declined with inactivation kinetics (τ_h = 210 $\pm$ 48 ms) identical to Kv1.3 (30, 31), and the pore blocker tetraethylammonium prevented inactivation (Fig. 5*A*, which is published as supporting information on the PNAS web site, www.pnas.org) indicative of C-type inactivation (32). With affinities identical to that for Kv1.3 (15–17, 23, 31), the K_V current was completely blocked by the selective Kv1.3 blocker, ShK-Dap^{22} (Fig. 1*C*), by the native ShK peptide (Fig. 5 *B* and *C*), and by three other peptide inhibitors (Fig. 1*D*). These data, taken together with an earlier report of Kv1.3 mRNA expression in PAS cells (6), indicate that the functional K_V channel in PAS cells is a homotetramer of Kv1.3 subunits.

Two components of K$^+$ current can be observed during voltage ramps in MBP-activated PAS cells dialyzed with 1 μM free Ca^{2+} in the pipette (Fig. 1*E*). At potentials more negative than -40 mV, Ca^{2+}-activated K$^+$ channel (K_{Ca}) currents activated rapidly after break-in, and at more depolarized potentials K$^+$ currents represented a combination of Kv1.3 and K_{Ca}. After blockade of Kv1.3 by ShK-Dap^{22}, the IKCa1 inhibitor TRAM-34 (21) blocked the residual K_{Ca} current (Fig. 1 *E* and *F*); the *Inset* in Fig. 1*E* shows the effect of TRAM-34 on an expanded scale. Complete inhibition of K$^+$ current by the combination of the two selective blockers strongly indicates that no additional K$^+$ chan-

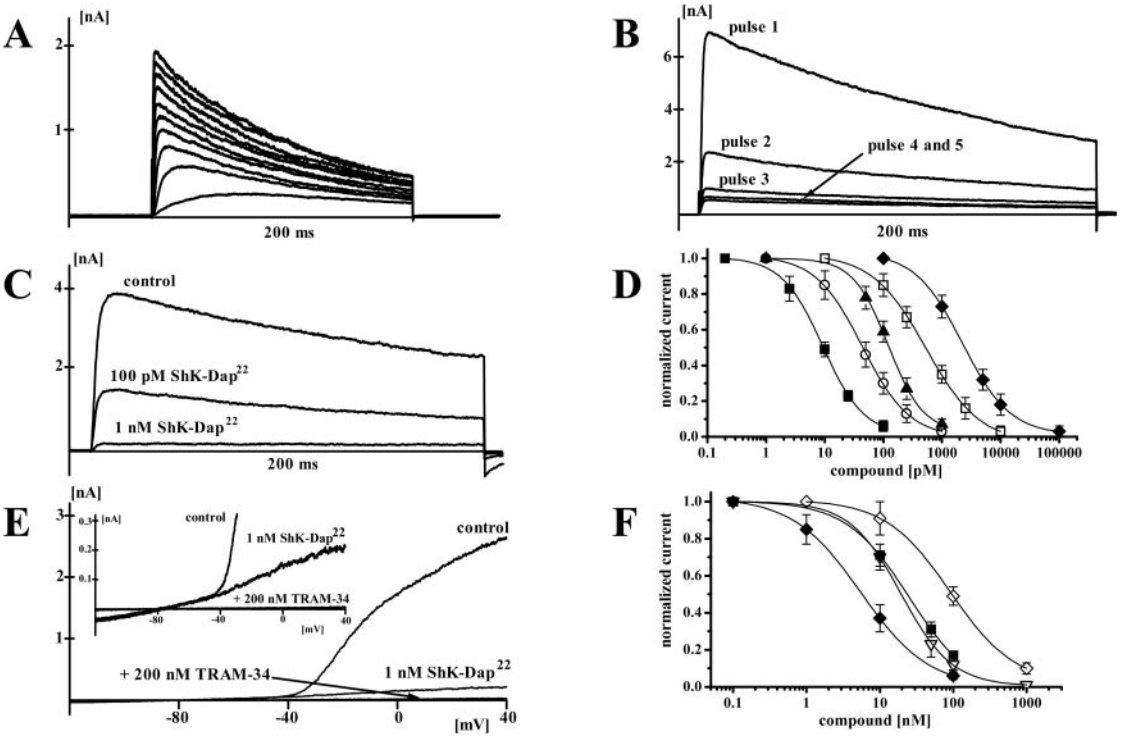

Fig. 1. Characteristics of the PAS T cell K_V and K_{Ca} channels. PAS cells were studied 48–72 h after MBP stimulation. (*A*) Family of K_V currents. The test potential was changed from −60 to +60 mV in 10-mV increments every 30 s ($V_{1/2} = -33$ mV). (*B*) Use-dependence. We used 200-ms pulses to 40 mV every second. (*C* and *D*) Pharmacology. Dose-dependent inhibition of K_V currents by ShK (■, $K_d = 9 \pm 0.8$ pM), ShK-Dap^{22} (○, $K_d = 45 \pm 6$ pM), MgTX (▲, $K_d = 125 \pm 12$ pM), KTX (□, $K_d = 532 \pm 72$ pM), and ChTX (◆, $K_d = 2.5 \pm 0.4$ nM). Every data point is the mean of three determinations. (*E*) K_V and IK currents during 200-ms ramp pulses and effect of 1 nM ShK-Dap^{22} and 200 nM TRAM-34 (*Inset*, 10 times scale). (*F*) Pharmacology. Dose-dependent inhibition of IK currents by ChTX (◆, $K_d = 5.5 \pm 1.1$ nM), TRAM-34 (▽, $K_d = 19 \pm 4$ nM), ShK (■, $K_d = 25 \pm 3$ nM) and clotrimazole (◇, $K_d = 91 \pm 9$ nM).

nels are present in PAS cells. With potencies identical to that for IKCa1 in human T cells (17, 21, 23), TRAM-34, clotrimazole, ChTX, and ShK blocked the K_{Ca} current in PAS cells. These data indicate that the functional K_{Ca} channel in MBP-activated PAS cells is IKCa1.

Four Channel-Defined Subsets in Rat T Cells. Fig. 2 (see also Fig. 6, which is published as supporting information on the PNAS web site) compares the functional expression levels for Kv1.3 and IKCa1 in rat T cells. Dividing the whole-cell Kv1.3 and IKCa1 conductance by the corresponding single-channel conductance determined the channel number per cell. Four general phenotypes are seen: "quiescent," "acutely activated," "transition," and "chronically activated." The quiescent population (no. 1 in Fig. 2) included unstimulated normal splenic or lymph node rat T cells that expressed 1–10 Kv1.3 and 10–20 IKCa1 channels per cell. The acutely activated subset comprised cells stimulated once or twice with mitogen (nos. 2–4) or antigen (no. 5) and expressed ≈200 Kv1.3 and ≈325 IKCa1 channels per cell (also see current traces in Fig. 5 *D–F*). The chronically activated group consisted of cells repeatedly activated (at least eight stimulations) with MBP (nos. 6–13) or with other antigens (nos. 14–16) and contained very high numbers of Kv1.3 (≈1500 per cell) and low to moderate numbers of IKCa1 (20–100 per cell). The transition group (nos. 19–25) comprised cells stimulated 3–6 times with antigen, had an intermediate phenotype, and may represent cells in the process of acquiring the chronically activated phenotype. This phenotypic change is illustrated by the CB cell line that expressed the acutely activated phenotype when stimulated for the first time *in vitro* with MBP (no. 5), but after 8–10 MBP-stimulations (nos. 9 and 10) expressed the chronically activated pattern (Fig. 2). Once acquired, the chronically acti-

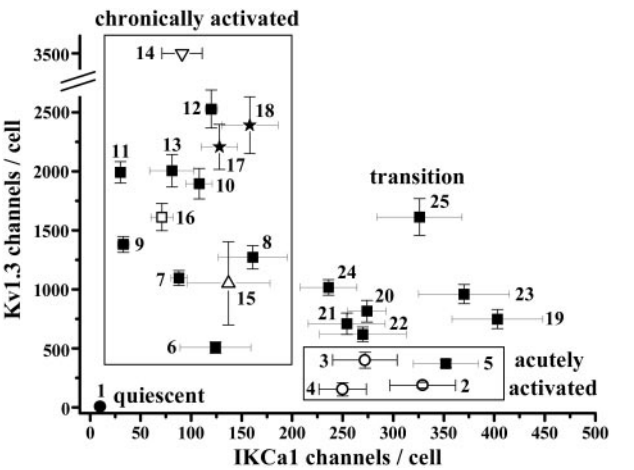

Fig. 2. Four channel-defined rat T cell subsets. Average numbers of Kv1.3 channels per cell ($n = 14$ to $36 \pm$ SEM) are plotted vs. average numbers of IKCa1 channels ($n = 10$ to 26). Activated T cells were studied 48–60 h after stimulation. Each cell line/clone or T cell population is numbered as follows. Quiescent group: quiescent normal rat T cells (no. 1). Acutely activated group: normal rat T cells stimulated once (no. 2) or twice with Con A (no. 3), or with PMA (phorbol 12-myristate 13-acetate) + ionomycin (no. 4); MBP-specific CB cells stimulated once with MBP (no. 5). Chronically activated group: T cell lines/clones stimulated ≥8 times by MBP:E10 (no. 6), MBP-33 (no. 7), LR88L1 (no. 8), CB8 (no. 9), CB10 (no. 10), Z (no. 11), PAS (no. 12), ZNP (no. 13); arthritogenic T cell clone (A2b) chronically activated with Mt (no. 14); T cell lines stimulated >8 times by ovalbumin (no. 15) or PPD (no. 16); chronically activated MBP-specific T cells restimulated with Con A:PAS (no. 17) and Z (no. 18). Transition population: T cell lines stimulated 3–6 times with MBP:DAG-S3 (no. 19), Go3-S3 (no. 20), Go1-S3 (no. 21), 71-S5 (no. 22), BP10-S5 (no. 23), Fischer S5 (no. 24), LEG-S6 (no. 25).

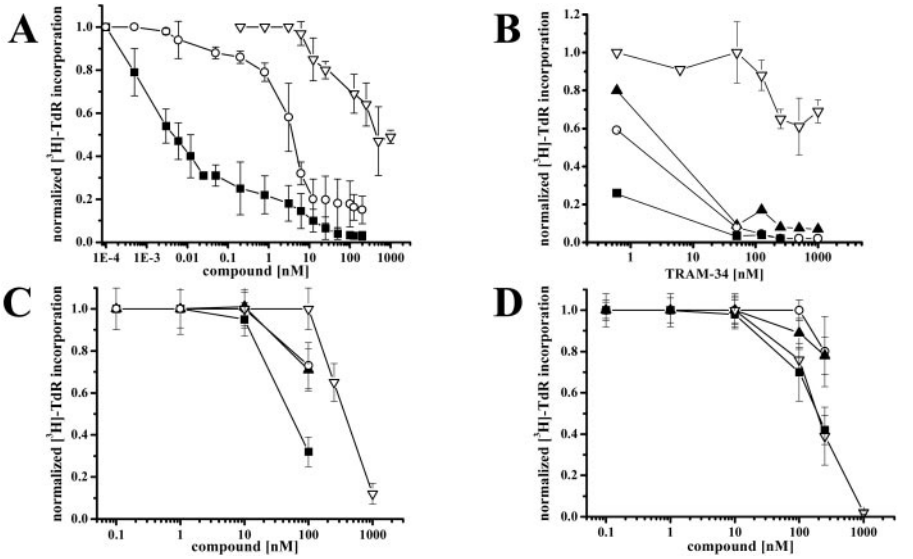

Fig. 3. Suppression of proliferation by K^+ channel blockers parallels channel phenotype. (*A*) Dose-dependent inhibition of [^{3}H]TdR incorporation in MBP-stimulated PAS cells. TRAM-34 (▽, $IC_{50} \approx 1$ μM), ShK (■, $IC_{50} = 30$ pM), and ShK-Dap^{22} (○, $IC_{50} = 1.4$ nM). Proliferation was also inhibited by the Kv1.3 blocker MgTX ($IC_{50} = 2$ nM, not shown). (*B*) Potentiation of the effects of TRAM-34 on MBP-stimulated PAS cells by combinations with ShK-Dap^{22}: TRAM-34 alone (▽, $IC_{50} \approx 1$ mM), TRAM-34 + 0.2 nM ShK-Dap^{22} (▲, $IC_{50} = 10$ nM), TRAM-34 + 0.4 nM ShK-Dap^{22} (○, 1.5 nM), TRAM-34 + 1.6 nM (■). (*C*) [^{3}H]TdR incorporation into quiescent normal rat T lymphocytes activated for 72 h with Con A in the presence or absence of channel blockers: TRAM-34 (▽, $IC_{50} = 375$ nM), ShK (■, $IC_{50} = 50$ nM), ShK-Dap^{22} (○), and MgTX (▲). (*D*) [^{3}H]TdR incorporation into Con A preactivated normal rat T cells that were restimulated with Con A for a further 72 h: TRAM-34 (▽, $IC_{50} = 200$ nM), ShK (■, $IC_{50} = 200$ nM), ShK-Dap^{22} (○), and MgTX (▲). Without stimulus, cpm values were <400 (*A* and *B*), <1,000 (*C*), and <8,000 (*D*); with stimulus, cpm values ranged from 100 to 250 $\times$ 10^3 (*A* and *B*), 30 $\times$ 10^3 (*C*), and 30–50 $\times$ 10^3 (*D*).

vated phenotype appears fixed because restimulation with Con A did not alter channel expression (nos. 17 and 18). Encephalitogenicity roughly correlated with the level of functional Kv1.3 expression, PAS (no. 12) and Z (no. 11) cells with the most Kv1.3 being most aggressive, and E10 (no. 6) with lower Kv1.3 numbers being less so. However, ZNP an MBP-activated clone derived from Z that had lost encephalitogenicity (no. 13), also showed high Kv1.3 expression. We conclude that chronically activated T cells, either disease inducing or innocuous, express a unique K^+ channel phenotype with highly up-regulated functional Kv1.3 expression.

Sensitivity to K^+ Channel Blockade in [^{3}H]TdR Incorporation Assays Parallels the Channel Phenotype. To investigate the requirement of Kv1.3 or IKCa1 for mitogen- or antigen-driven proliferation of the three major phenotypes, we studied the effects of selective Kv1.3 and IKCa1 blockade on MBP- or Con A-stimulated [^{3}H]TdR incorporation. The specific Kv1.3 blocker ShK-Dap^{22} potently suppressed MBP activation of chronically activated PAS cells, whereas ShK completely inhibited activation at picomolar concentrations paralleling its block of Kv1.3 (Fig. 1 *D* and *F* vs. Fig. 3*A*). In contrast, 1 μM TRAM-34, a concentration that blocks >95% of IKCa1 channels, only partially suppressed proliferation of PAS (Fig. 3*A*). Con A-stimulated [^{3}H]TdR incorporation by PAS cells was also suppressed by Kv1.3 (ShK-Dap^{22}, KTX, MgTX, and ShK) but not IKCa1 (TRAM-34) blockers (Fig. 7*A*, which is published as supporting information on the PNAS web site). Combined blockade of both channels produced greater inhibition than Kv1.3 blockade alone (Fig. 3*B*). In agreement with earlier reports on human cells (9, 33), K^+ channel blockade was not toxic as evidenced by trypan blue dye exclusion and propidium iodide staining (data not shown), and by the lack of suppression of IL-2-dependent proliferation (Fig. 7*B*).

In contrast to PAS cells, Con A activation of T cells with the quiescent phenotype was completely suppressed by 1 μM TRAM-34 ($IC_{50} \approx 375$ nM), whereas 100 nM ShK-Dap^{22} and MgTX (a concentration that would block >99% of Kv1.3) produced only 25% suppression (Fig. 3C). ShK suppressed Con A-stimulated proliferation of quiescent T cells only at high concentrations ($IC_{50} \approx 50$ nM) paralleling block of IKCa1 (Fig. 1 *D* and *F* vs. Fig. 3*C*). Similar results were obtained with acutely activated T cells. Con A-triggered [^{3}H]TdR incorporation was completely suppressed by 1 μM TRAM-34 ($IC_{50} \approx 200$ nM), whereas 100 nM ShK-Dap^{22} and MgTX produced only 20% suppression (Fig. 3*D*). ShK suppressed proliferation ($IC_{50} \approx 200$ nM) only at concentrations that block IKCa1 (Fig. 3*D*).

From these *in vitro* data, we conclude that proliferation of chronically activated encephalitogenic PAS cells depends primarily on Kv1.3, whereas proliferation of acutely activated normal rat T cells, like their human counterparts (10, 17), requires IKCa1. Quiescent rat cells are sensitive to IKCa1 but not Kv1.3 blockade, consistent with earlier reports that the membrane potential of rat and mouse T cells is determined by intermediate-conductance K_{Ca} (IK_{Ca}; ref. 34) and by an electrogenic Na^+K^+ pump, but not by Kv1.3 (18, 35). These results raise the possibility of selectively targeting the chronically activated encephalitogenic T cells by using Kv1.3 blockers without impairing the function of normal rat lymphocytes.

Disease Prevention and Treatment Trials. Based on the ability of selective Kv1.3 and IKCa1 blockers to inhibit proliferation in chronically and acutely activated T cells, respectively, we initiated animal trials to determine whether selective blockade of Kv1.3 and/or IKCa1 can prevent or treat AT-EAE in Lewis rats. As a first step by using a patch clamp bioassay, we determined that serum concentrations of 100 pM–14 nM for ShK and ShK-Dap^{22} were achieved within 15 min after i.p. and 30 min after s.c. injection. The average half-life was ≈20 min (Fig. 8, which is published as supporting information on the PNAS web site). Injection of 34 μg TRAM-34 (170 μg/kg i.p.) resulted in serum levels of 70–100 nM and an average half-life of ≈2 h (data not shown). Guided by these results, we embarked on prevention trials with exposure of PAS cells to blockers before (sensitization phase) and after adoptive transfer (effector phase) into animals.

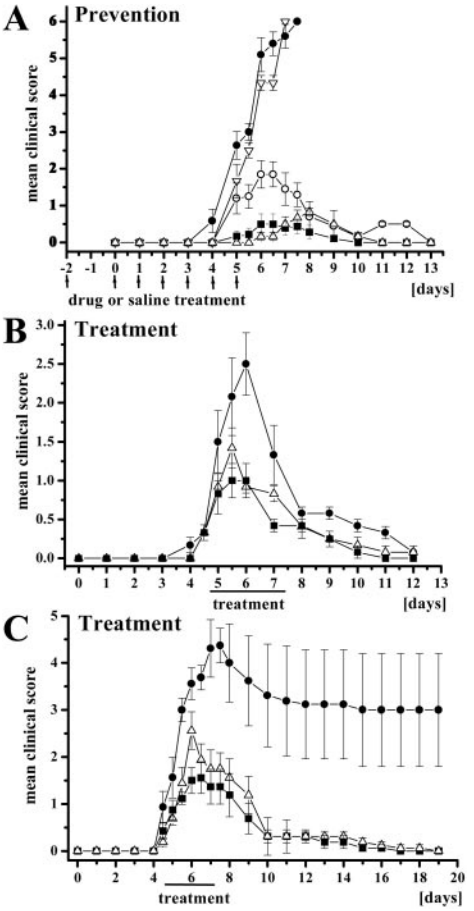

Fig. 4. Blockade of K^+ channels prevents and treats AT-EAE. Clinical scoring: 0 = no clinical signs, 0.5 = distal limp tail, 1 = limp tail, 2 = mild paraparesis or ataxia, 3 = moderate paraparesis, 4 = complete hind leg paralysis or severe ataxia, 5 = 4 + incontinence, 5.5 = tetraplegia, 6 = death. Mean ± SEM values are shown. *(A)* Prevention trial. PAS cells were activated *in vitro* (days −2 to 0) in the presence or absence of channel blockers and washed, and 4 or 5×10^6 viable cells were adoptively transferred i.p. on day 0. Rats were injected with saline (●) or K^+ channel blockers (▽, TRAM-34; ○, ShK-Dap^{22}; △, ShK-Dap^{22} + TRAM-34; ■, ShK) from day 0 to day 4 (as shown by the arrows below the *x* axis). For the control group, data are shown until day 7 when 10 of the 11 animals died; data beyond day 7 for the one surviving animal are not shown. (*B* and *C*) Treatment of moderate (*B*) and severe (*C*) EAE induced by different batches of PAS cells with varying encephalitogenic potencies. Rats were injected with saline or blockers for 3 days after the onset of clinical signs.

In subsequent treatment trials, drugs were administered exclusively *in vivo* after the onset of disease.

Our objective in the prevention trial was to compare results for selective Kv1.3 and IKCa1 blockers with previous results on KTX (blocks Kv1.3 and Kv1.1), by using an identical regimen (6). PAS cells were pretreated with channel blockers for 2 days *in vitro* before adoptive transfer of an equal number (4 or 5×10^6 in the two trials) of viable PAS cells into animals, and a series of injections then maintained channel blockade *in vivo* (Fig. 4*A* and Fig. 9 and Movies 1–12, which are published as supporting information on the PNAS web site). The 11 saline-control animals developed paralysis by day 5, and 10 died by day 8. In striking contrast, ShK greatly reduced disease severity, as did selective blockade of Kv1.3 by ShK-Dap^{22}. TRAM-34 alone had no effect, consistent with the channel phenotype and *in vitro* proliferation data, but it enhanced the effect of ShK-Dap^{22} when the two were administered together. Thus, specific pharmacological targeting of Kv1.3, alone or together with IKCa1, can prevent AT-EAE.

Can K^+ channel blockade reverse disease if initiated after the onset of clinical signs? To test therapeutic efficacy, the two drug combinations (ShK and ShK-Dap^{22} + TRAM-34) found to be most effective in the prevention trial were administered exclusively *in vivo* after the onset of disease (clinical score of 1.0). We titrated the degree of disease severity by using PAS cell batches with different encephalitogenic potencies and by adjusting the number of PAS cells transferred. In an experiment in which moderate disease was induced (maximum clinical score 2.5, Fig. 4*B*), ShK and the combination greatly reduced disease severity and ShK shortened its duration. In a second experiment (Fig. 4*C*), more severe disease (maximum mean clinical score 4.5) was induced; of eight control animals four died by day 7, and the remainder eventually recovered. Animals receiving ShK and the ShK-Dap^{22} + TRAM-34 combination showed improvement after 3 days of injections, and all survived (Fig. 4*B*). Data on individual animals are shown in Fig. 10, which is published as supporting information on the PNAS web site. In two additional experiments (data not shown) in which even more severe EAE was induced (100% mortality in the saline group), administration of ShK for 3 days after the onset of symptoms delayed progression of the disease for a time, but when treatment was withdrawn, most animals developed severe symptoms and died. The prevention and treatment trials together show the therapeutic potential of lymphocyte K^+ channel blockade in AT-EAE.

Discussion

By using whole cell recording, we have identified a unique channel phenotype in chronically activated T cells that is characterized by high expression of Kv1.3 channels (≈1500 per cell) along with low numbers of IKCa1 channels (≈120 per cell). This phenotype develops after at least eight repeated antigenic stimulations through a transition stage with intermediate channel numbers, and once acquired is not altered by restimulation with mitogen or antigen (Fig. 2). These cells may represent an expanded subset that normally exhibits the unique channel expression pattern, or they may have differentiated from naive T cells analogous to the development of central and effector memory T cells (36). This population included autoreactive disease-inducing T lymphocytes (several encephalitogenic MBP-specific T cell lines/clones and a single arthritogenic clone) as well as innocuous cells that had been repeatedly activated by ovalbumin or PPD. Within the MBP-specific T cells, the level of functional Kv1.3 expression roughly correlated with encephalitogenicity. Our data corroborate an earlier report that encephalitogenicity of the MBP-33 cell line (no. 7 in Fig. 2) parallels the expression of Kv1.3 but not the IL-2 receptor (37). Kv1.3 blockers potently suppressed antigen- or mitogen-stimulated proliferation of encephalitogenic cells, whereas IKCa1 blockade alone was ineffective (Fig. 3). Thus, the high Kv1.3/low IKCa1 channel expression pattern is a functionally relevant marker for chronically activated rat T lymphocytes.

We tested Kv1.3 and IKCa1 blockers in an animal model for MS. Lethal adoptive EAE was induced by $CD4^+$ MBP-specific chronically activated PAS T cells. Consistent with the patch-clamp and *in vitro* proliferation data, continuous and specific Kv1.3 blockade alone during *in vitro* activation and after transfer into animals effectively prevented severe AT-EAE, whereas selective IKCa1 block was ineffective. Simultaneous and highly selective blockade of both channels more effectively prevented disease. Exclusive *in vivo* administration of the two most effective drug injection regimens (ShK, ShK-Dap^{22} + TRAM-34) after the onset of symptoms ameliorated the clinical course of disease.

The highly potent marine product ShK was most effective in preventing lethal adoptive EAE and significantly ameliorated moderate and severe adoptive EAE when administered on

development of symptoms. ShK is the most potent inhibitor known for Kv1.3, and it also blocks IKCa1 and the neuronal channels Kv1.1, Kv1.4, and Kv1.6 (38). However, peak ShK blood levels after i.p injection (0.1–14 nM) are not sufficient to block IKCa1 channels. Direct and sustained blockade of neuronal channels by ShK to enhance conduction in demyelinated neurons and ameliorate paralysis is probably not involved in the *in vivo* effect because of the short half-life (≈20 min) of ShK. Thus, Kv1.3 in the immune system is likely to be the primary molecular target. In contrast to adoptive transfer EAE, active EAE triggered by guinea-pig myelin and complete Freund's adjuvant was not prevented by ShK (E. Mix, personal communication) or by KTX (E.B., unpublished data), most likely because this procedure induces T cells with the acutely activated phenotype. Because the arthritogenic rat T cell clone A2b expresses the chronically activated phenotype, ShK or ShK-Dap^{22} might also prove therapeutically effective in preventing adoptive autoimmune arthritis.

Although more experiments in chronic-relapsing EAE models are needed to evaluate Kv1.3 blockers both in rodents and primates, our findings suggest that ShK might represent a possible new therapeutic agent for MS, administered via the s.c. route like IFN-β (38) and glatiramer acetate (39). Our study also demonstrates high expression of Kv1.3 channels to be a general characteristic of chronically activated T cells, and we therefore propose Kv1.3 blockade to be a previously uncharacterized approach for the treatment of T cell-mediated autoimmune diseases.

This paper is dedicated to the memory of Professor Anna Mani, who passed away on August 16, 2001. We are deeply indebted to Drs. A. Ben-Nun, I. Cohen, D. Hinrich, S. Jung, F. Mor, and J. Whitaker for generously providing us with T cell lines and clones, without which our study would not have been possible. We thank Drs. J. M. Sabatier, Z. Fajloun, and I. Regaya for helping us in the MBP purification and the Centre de Formation et de Recherches Expérimental Medico-Chirurgicales for helping us in the animal experiments. This research was funded by grants from the National Multiple Sclerosis Society (K.G.C., E.B., M.D.C., and M.P.), the Association pour la Recherche sur La Sclérose en Plaques (E.B., C.B., and O.C.F.), the Fondation pour la Recherche Medicale (C.B.), the National Institutes of Health (MH59222 to K.G.C.; NS14069 to M.D.C.), and the Western States Affiliate of the American Heart Association (9920014Y to H.W.).

1. Hafler, D. A. & Weiner, H. L. (1995) *Immunol. Rev.* **144,** 75–107.
2. Ben-Nun, A. & Cohen, I. R. (1982) *J. Immunol.* **129,** 303–308.
3. Holoshitz, J., Naparstek, Y., Ben-Nun, A., Marquardt, P. & Cohen, I. R. (1984) *Eur. J. Immunol.* **14,** 729–734.
4. Genain, C. P., Roberts, T., Davis, R. L., Nguyen, M. H., Uccelli, A., Faulds, D., Li, Y., Hedgpeth, J. & Hauser, S. L. (1995) *Proc. Natl. Acad. Sci. USA* **92,** 3601–3605.
5. Heininger, K., Fierz, W., Schafer, B., Hartung, H. P., Wehling, P. & Toyka, K. V. (1989) *Brain* **112,** 537–552.
6. Beeton, C., Barbaria, J., Giraud, P., Devaux, J., Benoliel, A., Gola, M., Sabatier, J., Bernard, D., Crest, M. & Beraud, E. (2001) *J. Immunol.* **166,** 936–944.
7. Uccelli, A., Giunti, D., Mancardi, G., Caroli, F., Fiorone, M., Seri, M., Hauser, S. L. & Genain, C. P. (2001) *Eur. J. Immunol.* **31,** 474–479.
8. Negulescu, P. A., Shastri, N. & Cahalan, M. D. (1994) *Proc. Natl. Acad. Sci. USA* **91,** 2873–2877.
9. Cahalan, M. D. & Chandy, K. G. (1997) *Curr. Opin. Biotechnol.* **8,** 749–756.
10. Fanger, C. M., Rauer, H., Neben, A. L., Miller, M. J., Rauer, H., Wulff, H., Rosa, J. C., Ganellin, C. R., Chandy, K. G. & Cahalan, M. D. (2001) *J. Biol. Chem.* **276,** 12249–12256.
11. Fanger, C. M., Ghanshani, S., Logsdon, N. J., Rauer, H., Kalman, K., Zhou, J., Beckingham, K., Chandy, K. G., Cahalan, M. D. & Aiyar, J. (1999) *J. Biol. Chem.* **274,** 5746–5754.
12. Lewis, R. S. & Cahalan, M. D. (1995) *Annu. Rev. Immunol.* **13,** 623–653.
13. Khanna, R., Roy, L., Zhu, X. & Schlichter, L. C. (2001) *Am. J. Physiol.* **280,** C796–C806.
14. Price, M., Lee, S. C. & Deutsch, C. (1989) *Proc. Natl. Acad. Sci. USA* **86,** 10171–10175.
15. Leonard, R., Garcia, M., Slaughter, R. & Reuben, J. (1992) *Proc. Natl. Acad. Sci. USA* **89,** 10094–10098.
16. Kalman, K., Pennington, M. W., Lanigan, M. D., Nguyen, A., Rauer, H., Mahnir, V., Paschetto, K., Kem, W. R., Grissmer, S., Gutman, G. A., *et al.* (1998) *J. Biol. Chem.* **273,** 32697–32707.
17. Ghanshani, S., Wulff, H., Miller, M. J., Rohm, H., Neben, A., Gutman, G. A. & Cahalan, M. D. (2000) *J. Biol. Chem.* **275,** 37137–37149.
18. Koo, G. C., Blake, J. T., Talento, A., Nguyen, M., Lin, S., Sirotina, A., Shah, K., Mulvany, K., Hora, D., Jr., & Feeney, W. (1997) *J. Immunol.* **158,** 5120–5128.
19. Koo, G. C., Blake, J. T., Shah, K., Staruch, M. J., Dumont, F., Wunderler, D., Sanchez, M., McManus, O. B., Sirotina-Meisher, A., Fischer, P., *et al.* (1999) *Cell. Immunol.* **197,** 99–107.
20. Khanna, R., Chang, M. C., Joiner, W. J., Kaczmarek, L. K. & Schlichter, L. C. (1999) *J. Biol. Chem.* **274,** 14838–14849.
21. Wulff, H., Miller, M. J., Hänsel, W., Grissmer, S., Cahalan, M. D. & Chandy, K. G. (2000) *Proc. Natl. Acad. Sci. USA* **97,** 8151–8156.
22. Levite, M., Cahalon, L., Peretz, A., Hershkoviz, R., Sobko, A., Ariel, A., Desai, R., Attali, B. & Lider, O. (2000) *J. Exp. Med.* **191,** 1167–1176.
23. Rauer, H., Pennington, M., Cahalan, M. & Chandy, K. G. (1999) *J. Biol. Chem.* **274,** 21885–21892.
24. Deibler, G. E., Martenson, R. E. & Kies, M. W. (1972) *Prep. Biochem.* **2,** 139–165.
25. Beraud, E., Balzano, C., Zamora, A. J., Varriale, S., Bernard, D. & Ben-Nun, A. (1993) *J. Neuroimmunol.* **47,** 41–53.
26. Bourdoulous, S., Beraud, E., Le Page, C., Zamora, A., Ferry, A., Bernard, D., Strosberg, A. D. & Couraud, P. O. (1995) *Eur. J. Immunol.* **25,** 1176–1183.
27. Jung, S., Toyka, K. & Hartung, H. P. (1995) *Eur. J. Immunol.* **25,** 1391–1398.
28. Cahalan, M. D., Chandy, K. G., DeCoursey, T. E. & Gupta, S. (1985) *J. Physiol. (London)* **358,** 197–237.
29. Decoursey, T. E., Chandy, K. G., Gupta, S. & Cahalan, M. D. (1987) *J. Gen. Physiol.* **89,** 379–404.
30. Grissmer, S., Dethlefs, B., Wasmuth, J. J., Goldin, A. L., Gutman, G. A., Cahalan, M. D. & Chandy, K. G. (1990) *Proc. Natl. Acad. Sci. USA* **87,** 9411–9415.
31. Grissmer, S., Nguyen, A. N., Aiyar, J., Hanson, D. C., Mather, R. J., Gutman, G. A., Karmilowicz, M. J., Auperin, D. D. & Chandy, K. G. (1994) *Mol. Pharmacol.* **45,** 1227–1234.
32. Grissmer, S. & Cahalan, M. (1989) *Biophys. J.* **55,** 203–206.
33. Chandy, K. G., DeCoursey, T. E., Cahalan, M. D., McLaughlin, C. & Gupta, S. (1984) *J. Exp. Med.* **160,** 369–385.
34. Mahaut-Smith, M. P. & Mason, M. J. (1991) *J. Physiol. (London)* **439,** 513–528.
35. Ishida, Y. & Chused, T. M. (1993) *J. Immunol.* **151,** 610–620.
36. Sallusto, F., Lenig, D., Forster, R., Lipp, M. & Lanzavecchia, A. (1999) *Nature (London)* **401,** 708–712.
37. Strauss, U., Schubert, R., Jung, S. & Mix, E. (1998) *Recept. Channels* **6,** 73–87.
38. PRISMS Study Group (1998) *Lancet* **352,** 1498–1504.
39. Mancardi, G. L., Sardanelli, F., Parodi, R. C., Melani, E., Capello, E., Inglese, M., Ferrari, A., Sormani, M. P., Ottonello, C., Levrero, F., *et al.* (1998) *Neurology* **50,** 1127–1133.